Available online at www.sciencedirect.com
ScienceDirect
Optik 119 (2008) 203–208
Optik Optics
www.elsevier.de/ijleo

Effect of the parameters on diffraction efficiency after thermal fixing for reflection geometry hologram storage in $LiNbO_3$:Fe

Dongdong Teng[a], Biao Wang[b,a,*], Wei Yuan[a], Furi Ling Fu[b], Tao Geng[a]

[a]*Electro-Optics Technology Center, Harbin Institute of Technology, Harbin 150001, PR China*
[b]*Institute of Optoelectronic and Composite Materials/School of Physics and Engineering, Sun Yat-sen University, Guangzhou 510275, China*

Received 1 April 2006; accepted 31 July 2006

Abstract

For reflection geometry hologram storage in $LiNbO_3$:Fe, we have shown that the diffraction efficiency increases with doping level and thickness of storage material monotonically. When the acute angle between reference and z-axis is large enough for getting a relative small Bragg angle that is needed for angle multiplexing, smaller angle does good to diffraction efficiency after thermal fixing. And for absorption coefficient, there is an appropriate value responding to optimal diffraction efficiency after thermal fixing and we develop a theoretical model that predicts achievable diffraction efficiency after thermal fixing as a function of crystal thickness, doping level, acute angle between reference and z-axis and absorption coefficient. We compare this model with experiment results and get a good agreement.

Keywords: Absorption coefficient; Doping level; $LiNbO_3$:Fe; Diffraction efficiency; Thermal fixing

Volume holographic memory using photorefractive materials has become an important research focus that is pursued vigorously by many investigators for the potential in high-capacity storage and fast parallel readout. But for the practical realization, a reliable method for nondestructive readout of digital data must be demonstrated. A promising technique is thermal fixing [1] by compensation of mobile ion in photorefractive media and many investigations [2,3] have been done. In this paper, for multiplexed holograms storage in $LiNbO_3$:Fe, we have studied the influence of all parameters on the final diffraction efficiency after thermal fixing for reflection geometry.

As shown in Fig. 1, L is the thickness of recording material, θ is the acute angle between reference beam and z-axis in the recording material and c-axis is $\theta/2$ to z-axis. During hologram recording with extraordinary polarized light, the initial evolution of the local space-charge field can be obtained from the Kuktarev equation [4]. According to the analysis of Ref. [5], the first-order space-charge field could be expressed as

$$E_1(z) = m(z)E_{sc} \times \{1 - \exp[-t/\tau(z)] \exp[-jw_1(z)t]\},$$

where

$$m(z) = \frac{2\{S_0 \exp[-(\alpha/2)(L-z)]\}\{W_0 \exp[-(\alpha/2)z/\cos\theta]\}}{I_0(z)} \times \cos\theta,$$

*Corresponding author.
E-mail address: wangbiao@mail.sysu.edu.cn (B. Wang).

0030-4026/$ - see front matter © 2006 Elsevier GmbH. All rights reserved.
doi:10.1016/j.ijleo.2006.07.018

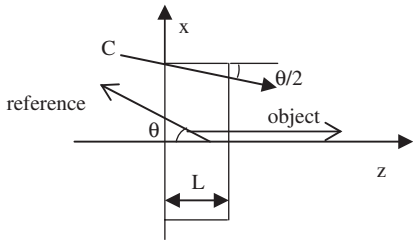

Fig. 1. Reflection geometry.

$$E_{sc} = E_q \left\{ \frac{E_{0ph}^2 + E_D^2}{\left[(N_A/N_D)E_{0ph}\right]^2 + (E_D + E_q)^2} \right\}^{1/2},$$

$$\tau_l(z) = \tau_{di}(z)\frac{1 + (E_D/E_\mu)}{1 + (E_D/E_q)} = \frac{\tau_x}{I_0(z)},$$

$$w_l(z) = \frac{1}{\tau_{di}(z)}\frac{N_A E_{0ph}}{N_D E_q}\frac{1}{1 + (E_D/E_\mu)}$$

and the parameters N_D is total Fe doping, N_A is initial Fe^{3+} concentration, dielectric relaxation time $\tau_{dl}(z) = (\varepsilon/q\mu)[\gamma_R N_A/sI_0(z)(N_D - N_A)]$, diffusion field $E_D = k_R TK/q$, saturation space-charge field $E_q = qN_A(N_D - N_A)/\varepsilon K N_D$, drift field $E_\mu = \gamma_R N_A/\mu K$ and photovoltaic field $E_{ph} = p\gamma_R N_A/q\mu s$. S_0 and W_0 are the signal and reference amplitudes at $z = 0$ and L, respectively, $I_0(z)$ is the local intensity, and α is the intensity absorption coefficient. The change of oxidation state affects terms N_A and the absorption coefficient α (proportional to $N_D - N_A$). The total Fe-doping N_D remains unchanged during annealing.

For exposure times much shorter than τ_l, including the absorption of the readout beam and scatting beam, the effective writing can write as

$$\left.\mathrm{d}\sqrt{\eta(t)}/\mathrm{d}t\right|_{t=0} = \frac{S_0 W_0 k_0 n_e^3 \left(r_{33}\cos^2\left(\frac{\theta}{2}\right) - \frac{n_0^4}{n_e^4} r_{13}\sin^2\left(\frac{\theta}{2}\right)\right)\cos(\theta)}{\alpha\tau_x} \times \exp\left(-\frac{\alpha}{2}L\right)\left[1 - \exp\left(-\frac{\alpha}{\cos\theta}L\right)\right]\frac{E_q\sqrt{E_{ph}^2 + E_D^2}}{E_D + E_q}.$$

During the erasure, the evolution of diffraction efficiency is

$$\eta(t) \propto \int_0^L \exp\left(-\frac{\alpha z}{\cos\theta}\right)\exp\left(-\frac{t}{\tau_x}I_0(z)\right)\mathrm{d}z \times \int_0^L \exp\left(-\frac{\alpha z}{\cos\theta}\right)\exp\left\{-\frac{t}{\tau_x} \times \left[S_0^2\exp(-\alpha(L - z)) + W_0^2\exp\left(-\frac{\alpha z}{\cos\theta}\right)\right]\right\}\mathrm{d}z$$

So the erasure time constants τ_e can be obtained approximately by

$$\frac{1}{\tau_e} = \frac{-(\mathrm{d}\eta/\mathrm{d}t)\big|_{t=0}}{\eta\big|_{t=0}} = \frac{1}{\tau_x}\left\{\frac{S_0^2}{1 - \cos\theta}\frac{\exp\left(-\frac{\alpha L}{\cos\theta}\right) - \exp(-\alpha L)}{\exp\left(-\frac{\alpha L}{\cos\theta}\right) - 1} + \frac{W_0^2}{2}\left[\exp\left(-\frac{\alpha L}{\cos\theta}\right) + 1\right]\right\}.$$

Therefore, the $M/\#$ in reflection geometry is

$$M/\# = \left(\mathrm{d}\sqrt{\eta(t)}/\mathrm{d}t\Big|_{t=0}\right) \times \tau_e. \tag{1}$$

Once the recording has been done, thermal fixing is needed for nondestructive readout of digital data. According to Ref. [6] and assuming that the electronic gratings are fully compensated by the proton grating after heating, which may be realize when the density of ions is sufficiently large, the thermal fixing efficiency under the short-circuit condition is denoted as

$$\eta_{fixing} = \frac{\left(\frac{N_D - N_A}{N_D}E_{ph}\right)^2 + E_D^2}{\left(\frac{N_D - N_A}{N_D}E_{ph}\right)^2 + (E_D + E_q)^2}. \tag{2}$$

Thus, for a large number of holograms M storage overlapped, the diffraction efficiency after thermal fixing can be expressed by

$$\eta = \left(\frac{M/\#}{M}\right)^2 \eta_{fixing} = \left\{\frac{S_0 k_0 n_e^3}{MW_0}\left[r_{33}\cos^2\left(\frac{\theta}{2}\right) - \frac{n_0^4}{n_e^4}r_{13}\sin^2\left(\frac{\theta}{2}\right)\right]\right\}^2 \times \left[\frac{1}{\alpha}\exp\left(-\frac{\alpha}{2}L\right)\right]^2\left[1 - \exp\left(-\frac{\alpha}{\cos\theta}L\right)\right]^4\left(\frac{E_q\sqrt{E_{ph}^2 + E_D^2}}{E_D + E_q}\right)^2 \times \left\{\frac{2(\cos\theta - 1)\cos(\theta)}{2\left(\frac{S_0}{W_0}\right)^2\left[\exp\left(-\frac{\alpha L}{\cos\theta}\right) - \exp(-\alpha L)\right] + (1 - \cos\theta)\left[\exp\left(-\frac{2\alpha L}{\cos\theta}\right) - 1\right]}\right\}^2 \times \frac{\left(\frac{N_D - N_A}{N_D}E_{ph}\right)^2 + E_D^2}{\left(\frac{N_D - N_A}{N_D}E_{ph}\right)^2 + (E_D + E_q)^2}. \tag{3}$$

According to the definition of these parameters, it can be gotten $E_D = 0.163/\Lambda$ and $E_q = 9.6 \times 10^{-9}\Lambda(N_A/N_D)(N_D - N_A)$ with $T = 300\,\mathrm{K}$ and $\Lambda = \lambda_0 \times 10^{-7}/(2n_e\cos(\theta/2))$. According to Refs. [7,8], the value of E_{ph} is a range from $10^{-15}N_A$ to $3 \times 10^{-14}N_A$ and here we take $10^{-14}N_A$.

For absorption coefficient α, research shows it is proportional to the density of filled traps [9]. By the study of Phillips and Staebler [10], to 0.001–0.1 mol% Fe-doped $LiNiO_3$, the amount of Fe ions per$\cdots cm^3$ is $1.89x \times 10^{20}$ for $x$mol% doping and especially $N_D - N_A = 1.51 \times 10^{17}\alpha$ for extraordinary light at

450 nm. For the study latter in this paper, 1.51×10^{17} is adopted for 488 nm approximately and other parameters are used include $r_{33} = 30.8 \times 10^{-12}$ m/V, $r_{13} = 8.6 \times 10^{-12}$ m/V, $n_e = 2.2446$, $n_0 = 2.20$ and $S_0^2 + W_0^2 = 110\,\mathrm{mV/cm^2}$. Actually the highest practical doping level is about 0.06 mol% limited by dark decay [11,12] and the angle θ is limited by not only geometrical light-path (a rather large θ is needed to make the diffracted data separate from the reflected light of reading light completely) and Bragg angle (when θ is too small, the Bragg angle is rather large and it is not good for hologram multiplexing) which decides the minimum value in practical experiment but also the refractivity of $LiNbO_3$ which decides the maximum value. Practically we take $5^\circ \leqslant \theta \leqslant 27^\circ$ in this paper.

With reference to Eq. (3), we study the diffraction efficiency η, which refers to the diffraction after thermal fixing for all this paper, as the function of S_0/W_0, L, α, θ and doping level. From the point of modulation depth, $m_0 = S_0/W_0 = 1$ is benefit for high dynamic range. In fact, this is correct even when absorption is considered for reflection geometry as shown in Fig. 2. And to all this paper, we take $m_0 = 1$ without noting.

As to the thickness of recording material, one observation from Fig. 3 is that the diffraction efficiency is monotone increasing with the increase of thickness when absorption coefficient is within the range that relatively better diffraction efficiency could be gotten. This is because for appropriate absorption coefficients the increasing of dynamic range is much more than the loss caused by the absorption for thicker material. But for reflection geometry reference beam is needed to cover object beam fully during the hologram recording processing and thus for high storage density the

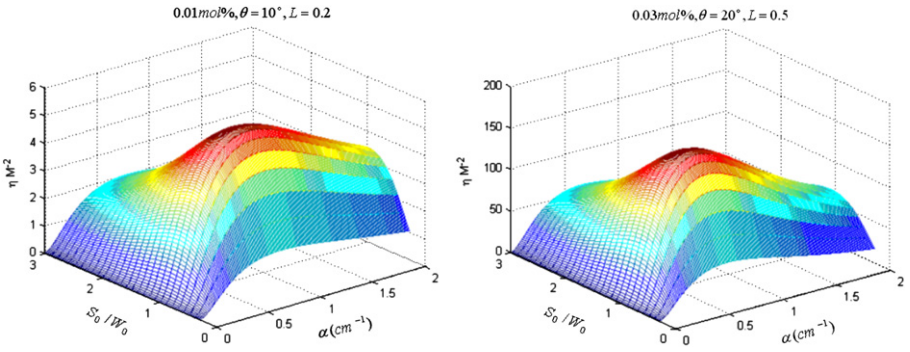

Fig. 2. Diffraction efficiency as a function of m_0 under different condition.

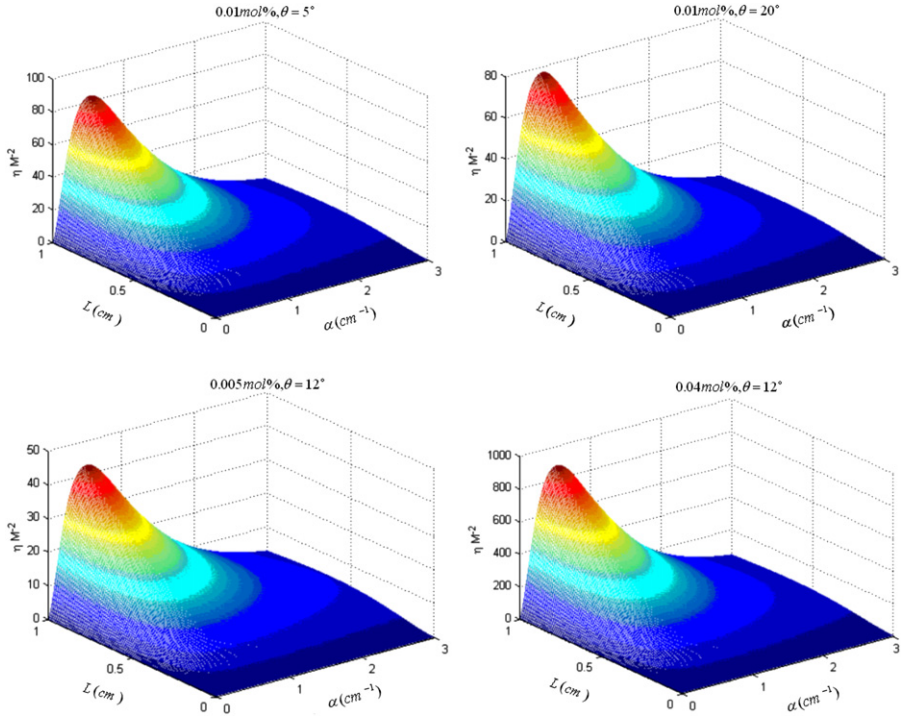

Fig. 3. Diffraction efficiency as a function of thickness of $LiNbO_3$:Fe.

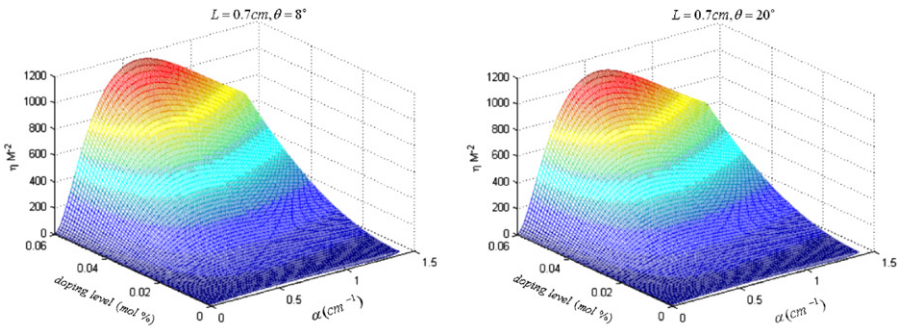

Fig. 4. Diffraction efficiency as a function of doping level with different θ and absorption coefficient.

thickness of recording material could not be too much. $L = 0.7$ cm is adopted for the rest of our study.

To the influence of doping level on diffraction efficiency, as shown in Fig. 4, our study gets the same result as that of thickness of $LiNbO_3$:Fe. Theoretically, diffusion field E_D is independent of doping level and saturation space-charge field E_q has little relationship with it except when doping level $\leqslant 0.005$ mol%. Thus, only photovoltaic field E_{ph} is normally proportional to doping level. So dynamic range is lager with high doping level. But thermal fixing efficiency has nothing with doping level because the influence of E_{ph} to fixing efficiency is rather little. Experimentally for the preparation of material, high doping level does harm to the optical quality of $LiNbO_3$:Fe. Generally moderate doping level, 0.01–0.03 mol% is favorable for hologram recording.

Without consideration of the minimum limitation of θ, it could be found the diffraction efficiency decreases with θ as shown in Fig. 5. Although E_q increases with θ, E_D decreases. The decisive effect of E_D makes the thermal fixing efficiency fall down with θ. For dynamic range, small value of θ leads to ideal modulation depth and could reduce the loss of light. So it falls down with θ, too. Thus these two factors lead to the monotonic degradation curve shown in Fig. 5.

The diffraction efficiency after thermal fixing is plotted in Fig. 6 as the function of absorption coefficient and θ with $5^\circ \leqslant \theta \leqslant 27^\circ$. It shows with the diminution of θ, the value of maximum diffraction efficiency increases with the corresponding absorption efficient between 0.5 and 1. According to Eq. (2), the thermal fixing efficiency decreases with absorption coefficient simply. But to dynamic range, the influence of absorption coefficient is a little sophisticated: a peak value of dynamic range is formed at a rather large absorption coefficient. This can be explained through Eq. (1): for dynamic range the two dominant terms are E_q, which increase with absorption, and $\exp(-\alpha L/2\cos\theta)$, which decreases with absorption. Intuitively, dynamic range is small for low absorption because the number of photogenerated electrons is small. But for higher absorption coefficient, the losses due to bulk absorption rapidly dominate, reducing the dynamic range. So the competing effect of bulk absorption and photorefractive dynamics leads to an absorption coefficient corresponding to the maximum dynamic range. Similarly for the diffraction efficiency after thermal fixing the value of absorption coefficient could be optimized for the best diffraction efficiency as the result of the completing between fixing factor and dynamic range factor (Fig. 7).

To verify the results of our calculation, we experimented the storage and thermal fixing of 500 holograms with different absorption coefficient with $L = 0.7$ cm, $m_0 = 1$, $\theta = 17^\circ$ (corresponding to 40° outside $LiNbO_3$:Fe) at 0.02 mol% doping level. The storage was carried out by angle multiplexing with a fixed object beam simplified as a parallel beam and 500 parallel reference beams in x–z plane with 0.03° (outside the $LiNbO_3$:Fe) separation around the reference beam of $\theta = 17^\circ$. Sequential exposure was adopted for equivalent diffraction efficiency. Then we heated the crystal to 150 °C for thermal fixing. The crystal was allowed to cool and illuminated with UV light to reveal the fixed holograms. After each diffraction efficiency measurement, the crystal was annealed at 980 °C in an argon–oxygen mixture. A combination of oxygen partial pressure and time was used as the control variable for changing the absorption coefficient measured at 488 nm extraordinary polarized light. No spatial variations in absorption coefficient were observed. Taking the diffraction efficiency corresponding to the reference beam of $\theta = 17^\circ$, Fig. 6 shows the comparing between experimental results and theoretical prediction. Exception that the experimental data is a little less than the prediction as a whole, it could be seen a good agreement between the theoretical prediction and the experimental data points. All the deviation could be explained as follows: (1) to the thermal fixing, the electronic gratings are not fully compensated by the proton grating after heating; (2) to angle multiplexing, the angle of references which is a range around $\theta = 17^\circ$ is different from our model taking θ as 17° exactly, (3) the coefficient of α to $N_D - N_A$ is not exactly for 488 nm.

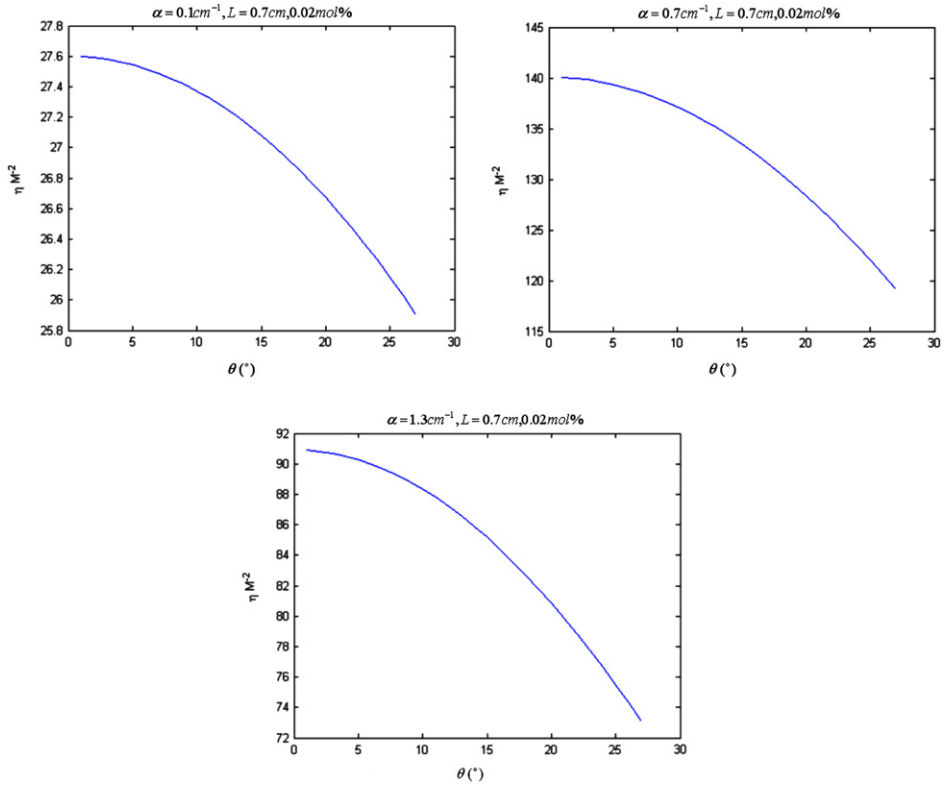

Fig. 5. Diffraction efficiency as a function of θ with different absorption coefficient at 0.02 mol% doping.

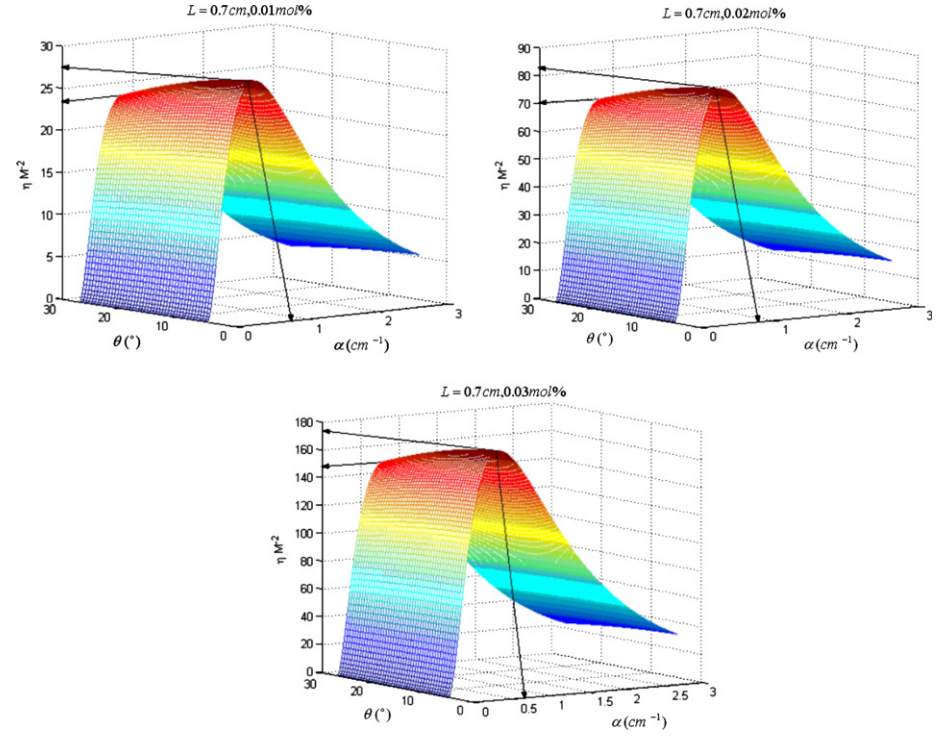

Fig. 6. Diffraction efficiency as a function of absorption coefficient and θ with different doping level.

In conclusion, from our study we know higher doping and thicker $LiNbO_3$:Fe are benefit for diffraction efficiency. Also the acute angle between reference and z-axis is better as small as possible, but too small angle would lead to a big Bragg angle which limits the angle multiplexing and do harm to the separation of diffracted

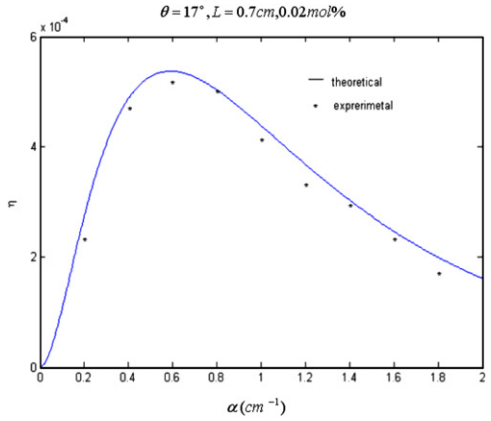

Fig. 7. Comparison of diffraction efficiency between experiment and theoretical prediction as a function of absorption coefficient.

light and reflected light of readout light. For moderate acute angle between reference and z-axis, an appropriate absorption coefficient is needed for optimal diffraction efficiency after thermal fixing and our model may predict this value effectively. This has a practical value for hologram storage including thermal fixing in $LiNbO_3$:Fe.

References

[1] J.J. Amodei, D.L. Staebler, Holographic pattern fixing in electro-optic crystals, Appl. Phys. Lett. 18 (1971) 540–542.

[2] M. Carrascosa, F. Agullo-lopez, Theoretical modeling of the fixing and developing of holographic gratings in $LiNbO_3$, Opt. Soc. Am. B 7 (1990) 2317–2322.

[3] X. An, D. Psaltis, G.W. Burr, Thermal fixing of 10,000 holograms in $LiNbO_3$:Fe, Appl. Opt. 38 (1999) 386–393.

[4] N.V. Kukhtarev, V.B. Markov, S.G. Odulov, M.S. Soskin, V.L. Vinetskii, Holographic storage in electro-optic crystals I steady state, Ferroelectrics 22 (1979) 949–960.

[5] C. Gu, J. Hong, H. Li, D. Psaltis, P. Yeh, Dynamics of grating formation in photovoltaic media, J. Appl. Phys. 69 (3) (1991) 1167.

[6] A. Yariv, S. Orlov, G. Rakuljic, V. Leyva, Holographic fixing, readout, and storage dynamics in photorefractive materials, Opt. Lett. 20 (1995) 1334–1336.

[7] D.L. Staebler, Holographic Recording Materials, in: H.M. Smith (Ed.), Topics in Applied Physics, Vol. 20, Springer, Berlin, 1977, pp. 101–132.

[8] A. Glass, D.V. Linde, T.J. Negram, High-voltage bulk photovoltaic effect and the photorefractive process in $LiNbO_3$, Appl. Phys. Lett. 25 (4) (1974) 233.

[9] E. Krätzig, R. Orlowski, Light induced charge transport in doped $LiNbO_3$ and $LiTaO_3$, Ferroelectrics 27 (1980) 241–244.

[10] W. Phillips, D.L. Staebler, Control of the Fe^{2+} concentration in iron-doped lithium niobate, J. Electron. Mater. 3 (2) (1974) 601.

[11] Y. Yang, I. Bee, K. Buse, D. Psaltis, Ionic and electronic dark decay of holograms in $LiNbO_3$:Fe crystals, Appl. Phys. Lett. 78 (2001) 4076–4078.

[12] I. Nee, M. Müller, K. Buse, E. Krätzig, Role of iron in lithium-niobate crystals for the dark-storage time of holograms, J. Appl. Phys. 88 (2000) 4282–4286.